

See discussions, stats, and author profiles for this publication at: <https://www.researchgate.net/publication/269766866>

One Platform Comparison of Estrone and Folic Acid Anchored Surface Engineered MWCNTs for Doxorubicin Delivery

ARTICLE in MOLECULAR PHARMACEUTICS · DECEMBER 2014

Impact Factor: 4.38 · DOI: 10.1021/mp500720a · Source: PubMed

CITATIONS

6

READS

38

2 AUTHORS:



Neelesh Mehra

Texas A&M University - Kingsville

49 PUBLICATIONS 457 CITATIONS

[SEE PROFILE](#)



Narendra K Jain

ISF College of Pharmacy

302 PUBLICATIONS 8,854 CITATIONS

[SEE PROFILE](#)

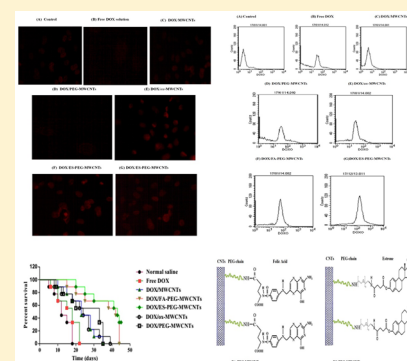
One Platform Comparison of Estrone and Folic Acid Anchored Surface Engineered MWCNTs for Doxorubicin Delivery

Neelesh Kumar Mehra^{†,‡} and N. K. Jain*,^{†,‡}

[†]Pharmaceutics Research Laboratory, Department of Pharmaceutical Sciences, Dr. H. S. Gour University, Sagar 470 003, India

[‡]Pharmaceutical Nanotechnology Research Laboratory, ISF College of Pharmacy, Moga 142 001, India

ABSTRACT: Our main aim in the present investigation was to assess and compare the *in vitro* and *in vivo* cancer targeting propensity of doxorubicin (DOX) loaded folic acid (FA) and estrone (ES) anchored PEGylated multiwalled carbon nanotubes (MWCNTs) employing tumor bearing Balb/c mice. The DOX was loaded into the developed functionalized MWCNTs after proper characterization using dialysis diffusion method. The *in vitro*, *ex vivo*, and *in vivo* studies were performed on the MCF-7 cell line for assessment of the cancer targeting propensity. Both qualitative and quantitative cell uptake studies indicated the preferential higher uptake of estrone anchored nanotube formulation compared to other formulations and free DOX owing to the overexpression of estrogen receptors (ERs) on human breast MCF-7 cells. Similarly, the pharmacokinetic and increased antitumor activities also confirmed the elevated cancer targeting propensity of the estrone and folic acid anchored MWCNT formulations. The DOX/ES-PEG-MWCNTs has also shown significantly longer survival span (43 days) than free DOX (18 days) and control group (12 days). Present outcomes from the *ex vivo* and *in vivo* studies are deemed to be of great scientific value and shall assist targeted drug delivery formulation scientists for selection of the targeting moieties in the treatment of human breast cancer.



KEYWORDS: carbon nanotubes, drug targeting, doxorubicin, pharmacokinetic, breast cancer, estrone, folic acid, antitumor activity

1. INTRODUCTION

On recalling the “*Magic bullet concept*” tremendous sophistication has been visualized in targeting concepts and delivery of bioactives. In the present scenario, carbon nanotubes (CNTs) have attracted escalating attention after attachment of huge targeting moieties to offer sustained/controlled release behavior with cellular targeting and enhanced specificity.^{1,2}

CNTs were first discovered and fully explored in 1991.³ CNTs are unique, three-dimensional sp² hybridized carbon nanomaterials that have attracted tremendous attention as a valuable, promising, safe and effective alternative nanoarchitecture for biomedical applications due to their unique physicochemical properties such as biocompatibility, non-immunogenicity, high loading efficiency, high aspect ratio, structural flexibility, and nontoxic nature.^{2–9} Functionalized CNTs (*f*-CNTs) have the capacity to readily cross the plasma membrane via an energy-dependent, endosomally mediated and direct translocation, which is known as tiny nanoneedle mechanism.^{9,10} Due to the tiny nanoneedle tubular shape, they pass through cell membrane without causing cell death, thus allowing efficient tissue and tumor specific drug delivery with minimal or no toxic effects. Compared with other nanocarrier systems, which have low entrapment efficiency due to steric hindrance, the *f*-CNTs have greater entrapment due to the availability of high surface area.^{4,11,12}

Despite excellent progress in using surface engineered CNTs as targeted drug delivery carriers, more research is needed to further optimize their ability to selectively accumulate in

diseased/targeted tissues and to release their toxic payload in a controlled manner. To date, numerous research reports are available considering functionalized CNTs for drug delivery including doxorubicin hydrochloride,^{13–15} paclitaxel,¹⁶ docetaxel,¹⁷ gemcitabine,¹⁸ amphotericin B,¹⁹ gliotoxin,²⁰ sulfasalazine,²¹ oxaliplatin,²² etc.

The anthracycline antibiotic, doxorubicin hydrochloride, chosen for the present investigation as an anticancer agent is widely used in the treatment of cancers of the breast, prostate, brain, and cervix and Hodgkin lymphoma. Short half-life and severe toxicity (acute cardiotoxicity) associated with doxorubicin restrict its clinical application. According to the Biopharmaceutical Classification System (BCS) doxorubicin hydrochloride belongs to class III, i.e., high solubility and low permeability (BCS III). BCS is a scientific framework for classifying substances according to their aqueous solubility and permeability.^{23–25} Very recently our laboratory explored the delivery of DOX employing D- α -tocopheryl polyethylene glycol 1000 succinate (TPGS) as targeting ligand with improved therapeutic outcomes and antitumor targeting efficacy on the MCF-7 cell line.⁴ The purpose of the present investigation was to compare the cancer-targeting propensity of the folic acid (FA) and estrone (ES) appended surface functionalized

Received: October 27, 2014

Revised: December 13, 2014

Accepted: December 17, 2014

Published: December 17, 2014

MWCNTs employing breast cancer cells on Balb/c mice. The cancerous cells overexpress the folate receptors (FRs) and estrogen receptors (ERs) belonging to folate and nuclear hormone receptor superfamily, respectively.²⁶ The MWCNTs tethering ES and FA probably deliver DOX more efficiently into the cancerous cells after binding selectively to their respective receptors through endocytosis or tiny nanoneedle mechanism. The ligand-driven MWCNTs are an established, well-known concept, and these targeting moieties can be easily attached to *f*-MWCNTs. The comparative cancer targeting propensity of targeting ligand conjugated *f*-MWCNTs studied on a single platform reported herein is expected to be of greater scientific interest in targeted drug delivery. We have extensively characterized the ligand (ES and FA) conjugated MWCNTs *in vitro*, *ex vivo*, and *in vivo* in terms of biodistribution and pharmacokinetics, Kaplan–Meier survival analysis, and tumor targeting efficacy on Balb/c mice.

2. MATERIALS AND METHODS

2.1. Materials. Multiwalled carbon nanotubes (MWCNTs) produced by chemical vapor deposition (CVD) with purity 99.3% were purchased from Sigma-Aldrich Pvt. Ltd. (St. Louis, Missouri, USA). Doxorubicin hydrochloride was received as a benevolent gift from M/s Sun Pharm Advanced Research Centre (SPARC), Vadodara, India. Folic acid (FA), dimethyl sulfoxide (DMSO), 1-ethyl-3-(3-dimethylaminopropyl)-carbodiimide (EDC), and dialysis membrane (MWCO, 5–6 kDa) were purchased from HiMedia Pvt. Ltd. Mumbai, India. Estrone (ES) was purchased from Sigma-Aldrich Pvt. Ltd. USA. All the reagents and solvents were used as received.

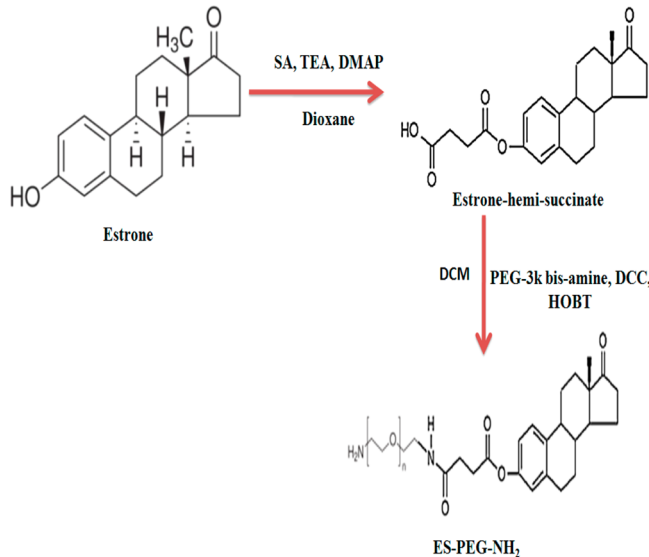
2.2. Functionalization of MWCNTs. The procured pristine MWCNTs were initially purified and treated with strong oxidizing acid following a previously reported method from our and other laboratories after minor modifications.^{2,4,10,13,27,28} Briefly, MWCNTs (500 mg) were treated with concentrated nitric acid and sulfuric acid ($\text{HNO}_3:\text{H}_2\text{SO}_4::1:3$) mixture with continuous magnetic stirring at 100 rpm (Remi, Mumbai, India) maintaining $100 \pm 5^\circ\text{C}$ temperature for 24 h. Then dispersed MWCNTs were washed with deionized water, ultracentrifuged, vacuum-dried, and collected. Treated MWCNTs (300 mg) were further treated with ammonium hydroxide (NH_4OH) and hydrogen peroxide (H_2O_2) in 50:50 ratio in a round-bottom flask (RBF) at $80 \pm 5^\circ\text{C}$ for 24 h. The treated oxidized MWCNTs (*ox*-MWCNTs) were repeatedly washed to neutral pH, ultracentrifuged (Z36HK, HERMLE LaborTechnik GmbH, Germany) at 20,000 rpm for 15 min, and finally lyophilized (Heto dry Winner, Germany).

2.3. Conjugation of Estrone to Surface Functionalized MWCNTs (ES-PEG-MWCNTs). The conjugation of estrone (ES) with oxidized-MWCNTs was performed using standard 1-ethyl-3-(3-dimethylaminopropyl)carbodiimide (EDC) chemistry in three steps following the previously reported methods after minor modifications.^{23,27,29}

2.4. Activation of Estrone. Briefly, estrone (ES; 8 mM), succinic anhydride (SA; 10 mM), dimethylaminopyridine (DMAP; 8 mM), and triethylamine (TEA; 8 mM) were dissolved in dioxane and magnetically stirred overnight at $25 \pm 2^\circ\text{C}$. The dioxane was evaporated under vacuum, and the obtained residue was dissolved in dichloromethane (DCM) and filtered. The filtrate was further dried and precipitated using diethyl ether to obtain the carboxylic acid derivative of estrone (ES-COOH). The ES-COOH (0.5 mM) was dissolved in

DCM (0.5 mM) in equimolar concentration, and hydroxybenzotriazole (HOBT; 0.1 mM), PEG-3000-amine, and DCC were added to it and continually magnetically stirred at $25 \pm 2^\circ\text{C}$ for 24 h until precipitate was formed. The pellet of ES-PEG-NH₂ was collected by centrifugation (Scheme 1), repeatedly washed with deionized water, and collected.^{23,30}

Scheme 1. Conjugation of PEG to Activated Estrone



The COOH-MWCNTs (33.36 mg) and EDC (6.41 mg) were dissolved in DMSO with continuous magnetic stirring at 100 rpm. After 6 h, ES-PEG-NH₂ in DMSO (4.60 mg/mL) solution was added and kept magnetic stirred up to 5 days. Then the unreacted biproducts/materials were separated out, lyophilized (Heto dry Winner, Denmark, Germany), collected, and stored (Scheme 2).²⁷

2.5. Synthesis of FA-PEG Conjugation to Functionalized MWCNTs. The *tert*-butoxycarbonyl (*t*-Boc)-protected folic acid (FA) for amine protection of FA was synthesized, and its further activation was performed following the previously reported well-known method to obtain *t*-Boc-FA-NHS.^{2,31}

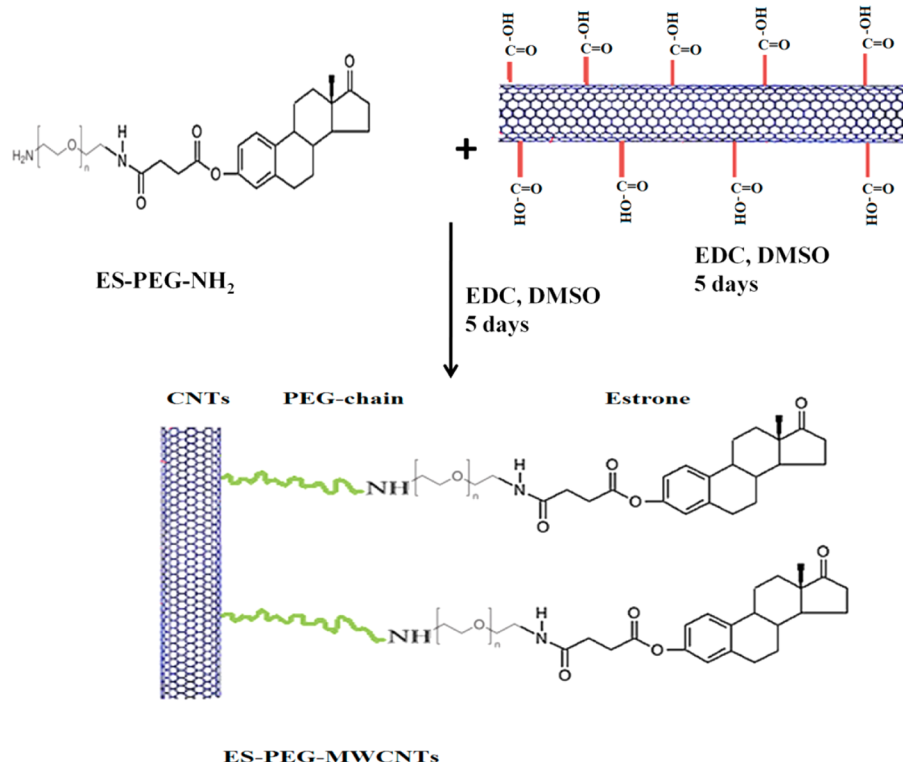
2.5.1. Conjugation of *t*-Boc-FA to Surface Functionalized MWCNTs. The *t*-Boc-FA-NHS (16.25 mg) was mixed with PEG-3k bis amine (Sigma-Aldrich, USA) (225.0 mg) in DMSO in the presence of triethylamine (TEA) and magnetically stirred for 24 h at $25 \pm 2^\circ\text{C}$. The obtained *t*-Boc-FA-PEG-NH₂ as a pale yellow solid was collected and dried.

The *t*-Boc-FA-PEG-NH₂ was mixed with *ox*-MWCNTs in DMSO followed by addition of EDC and continually magnetically stirred for 5 days maintaining the dark condition at $25 \pm 2^\circ\text{C}$ (Scheme 3). The resultant conjugate was collected, dried, and characterized by FTIR spectroscopy.^{2,10,32}

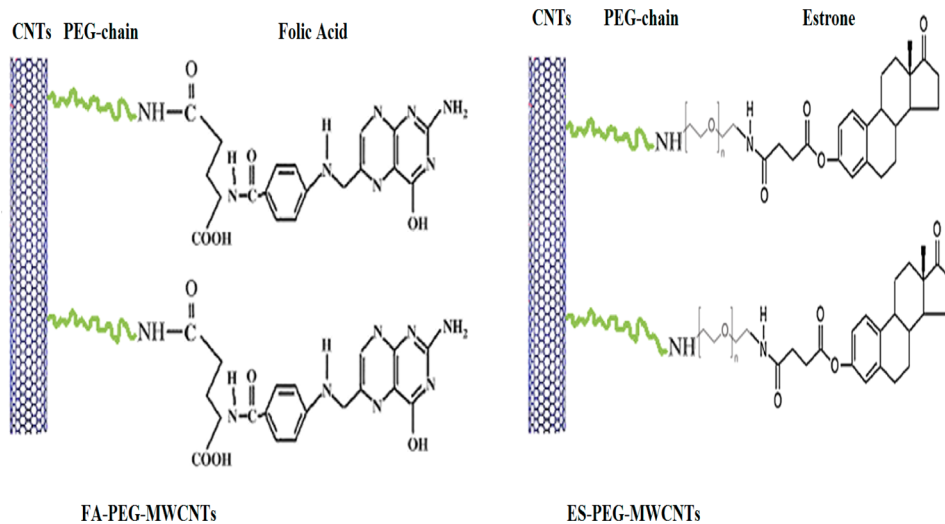
The activation and conjugation of both ligands with MWCNTs were extensively characterized by UV-vis spectroscopy (Shimadzu 1601, UV-visible spectrophotometer, Shimadzu, Japan), and Fourier transform infrared spectroscopy (FTIR) was performed using the KBr pellet method (PerkinElmer 783, Pyrogon 1000 spectrophotometer, USA) scanned in the range from 4000 to 500 cm^{-1} .

2.6. Characterization of the MWCNT Conjugates. The developed MWCNT conjugates were characterized for particle size by photon correlation spectroscopy in a Malvern Zetasizer nano ZS90 (Malvern Instruments, Ltd., Malvern, U.K.) at room

Scheme 2. Development of ES-PEG-MWCNT Conjugate



Scheme 3. Conjugation Scheme of FA-PEG and ES-PEG Conjugated MWCNTs



temperature, atomic force microscope (AFM) using Digital Nanoscope IV Bioscope (Veeco Innova Instruments, Santa Barbara, CA, USA), FTIR spectroscopy using PerkinElmer FTIR spectrophotometer (PerkinElmer 783, Pyrogon 1000 Spectrophotometer, Shelton, Connecticut), ¹H nuclear magnetic resonance (NMR) spectroscopy (Bruker, DRX, USA), and Raman spectroscopy RINSHAW, inVia Raman spectrophotometer (Renishaw, Gloucestershire, U.K.).

2.7. DOX Loading Studies. DOX was loaded into the MWCNT dispersion using modified equilibrium dialysis method as reported previously.^{10,15,25} Briefly, DOX was initially dissolved in acetone, and aqueous triethylamine (TEA) solution was added in a 2:1 molar ratio (DOX:TEA). The DOX was magnetically stirred (100 rpm; Remi, India) with the

developed MWCNT conjugates and pristine MWCNTs in phosphate buffer solution (PBS: pH 7.4) using Teflon beads overnight at 37 ± 0.5 °C for 24 h to facilitate DOX loading. MWCNT conjugates were then ultracentrifuged until the nanotube dispersion became color free. The amount of unbound DOX was determined measuring absorbance at λ_{max} 480.2 nm spectrophotometrically (Shimadzu 1601, UV-visible spectrophotometer, Shimadzu, Japan). The developed DOX loaded MWCNT (DOX/MWCNTs, DOX/ox-MWCNTs, DOX/ES-PEG-MWCNTs, and DOX/FA-PEG-MWCNTs) conjugates were collected, dried, lyophilized (Heto dry Winner, Denmark, Germany), and stored at 2–8 °C for further use. The DOX loading efficiency (%) was calculated using the following formula:

$$\% \text{ loading efficiency} = \frac{\text{wt of loaded DOX} - \text{wt of free DOX}}{\text{wt of loaded DOX}} \times 100$$

2.8. In Vitro Release Studies. The dispersion of DOX/MWCNT, DOX/*ox*-MWCNT, DOX/ES-PEG-MWCNT, and DOX/FA-PEG-MWCNT conjugates was studied in sodium acetate buffer saline (pH 5.3) and phosphate buffer saline (pH 7.4) as recipient media using a modified dissolution method with maintenance of 37 ± 0.5 °C physiological temperature. The MWCNT conjugates were filled in pretreated dialysis membrane (MWCO 5–6 kDa, HiMedia, Mumbai, India) separately and kept in the releasing media under constant magnetic stirring (100 rpm; Remi, Mumbai, India) at 37 ± 0.5 °C. At definite time points, the MWCNT samples were withdrawn, and after each sampling, the withdrawn medium was replenished with fresh sink solution maintaining strict sink condition. The drug concentration was determined after proper dilution in a UV/visible spectrophotometer at λ_{max} 480.2 nm (UV/vis, Shimadzu 1601, Kyoto, Japan).

2.9. Ex Vivo (Cell Line) Studies. The *ex vivo* (cell line) studies were performed on Michigan Cancer Foundation human breast cancer cells (MCF-7) cell line procured from National Center for Cell Sciences (NCCS), Pune, India. The MCF-7 cells were maintained in Dulbecco's modified Eagle's medium (DMEM; HiMedia, Mumbai, India) containing 10% fetal bovine serum (FBS; Sigma, St. Louis, Missouri) supplemented with 1% antibiotic (penicillin–streptomycin) solution grown to confluence in humidified atmosphere containing 5% CO₂ at 37 °C. Cells were seeded at a density of 4×10^3 cells/well and incubated for 24 h prior to commencement of the experiments. The DMEM medium was changed as per requirement every alternate day, and cells with approximately 80% confluence were used for further studies. After that, medium was decanted and washed with fresh PBS (6 mL for 25 cm²) and cells were trypsinized using 0.25% trypsin solution. Trypsin was removed completely, and subsequently medium was added to split the cells.^{4,14}

2.10. Cell Viability Assay. The cell viability assay was performed using 3-(4,5-dimethylthiazol-2-yl)-2,5-diphenyltetrazolium bromide (MTT) dye reduction assay to a blue formazan derivative by living cells to assess the cytotoxic propensity of the nanotube formulations at different concentrations.^{27,28,33} Briefly, MCF-7 cells were placed onto 96-well flat-bottomed tissue culture plates (Sigma, Germany) and allowed to adhere for 24 h at 37 °C prior to assay. The cells in quadruplicate were treated with free DOX, DOX/MWCNTs, DOX/*ox*-MWCNTs, DOX/FA-PEG-MWCNTs, and DOX/ES-PEG-MWCNTs with increasing concentration (0.001–100 μM) of DOX simultaneously under controlled environment for 24 and 48 h at 37 ± 0.5 °C in a humidified atmosphere with 5% CO₂. Thereafter, medium was decanted and 50 μL of methylthiazole tetrazolium (MTT; 1 mg/mL) in DMEM (10 μL; 5 mg/mL in Hanks balanced salt solution; without phenol red) was added to each well and incubated for 4 h at 37 °C. Formazan crystals were solubilized in 50 μL of isopropanol by shaking at rt for 10 min. The absorbance was taken using a microplate reader (Medispec Ins. Ltd., Mumbai, India) at 570 nm wavelength, blanked with DMSO solution, and (%) cell viability was calculated using the following formula:

$$\text{cell viability (\%)} = \frac{[A]_{\text{test}}}{[A]_{\text{control}}} \times 100$$

where [A]_{test} is the absorbance of the test sample and [A]_{control} is the absorbance of control samples.

2.11. Cell Uptake Study. Cellular uptake studies were carried out through flow cytometry analysis using FACS Calibur flow cytometer (Becton, Dickinson Systems, FACS canto, USA) on MCF-7 cell line to determine the intracellular uptake efficiency of the developed surface engineered MWCNT formulations.^{20,27,34–36} The cellular uptake of free DOX and DOX loaded MWCNT formulations using MCF-7 cell line was performed through flow cytometry. The cell suspension was incubated at 25 ± 2 °C for 4 h with intermittent mixing every 20 min. The 4×10^3 cells per well were seeded in a 12-well plate and incubated for 24 h at 37 ± 0.5 °C with 5% CO₂, and then the medium in each well was replaced with 2 mL of serum-free and antibiotic-free medium. Then various concentrations of MWCNT formulations (DOX solution, DOX/MWCNTs, DOX/*ox*-MWCNTs, DOX/FA-PEG-MWCNTs, and DOX/ES-PEG-MWCNTs) were incubated for 3 h. Three hours post *in vitro* incubation, cells were washed three times with ice-cold PBS, trypsinized (0.1%; w/v), pelletized via centrifugation (1000g) to remove the trypsin, and finally resuspended in PBS. Cells associated with DOX were measured quantitatively (FACS Calibur flow cytometer; Becton, Dickinson Systems, FACS canto, USA) and qualitatively (fluorescence microscope, Leica, Germany).

2.12. Cell Cycle Distribution Measurement. The DNA content in the different cell cycle phases was determined by flow cytometry for 24 h after treatment with the developed MWCNT formulations.^{4,37–39} Briefly, 4×10^3 cells were seeded and allowed to attach overnight at 37 ± 0.5 °C; the cultured cells were treated with developed optimized nanotube formulation (2 nM/mL concentration of drug) under CO₂ atmosphere, and the incubated cells were harvested, washed, and fixed using 70% cold ethanol overnight. Subsequently the cells were trypsinized, washed again, fixed, and further resuspended in hypotonic propidium iodide solution (PI; 50 μg/mL) containing ribonuclease A (RNase free, 100 μg/mL) and incubated for 30 min at 37 °C in dark before measurement. The distribution of cell cycle was determined with FACS Calibur flow cytometer and analyzed using Cell Quest software (Becton, Dickinson Systems, FACS canto, USA).

2.13. In Vivo Studies. **2.13.1. Animals and Dosing.** The Balb/c mice of either sex (20–25 g) were used for *in vivo* studies, as mice present a more sensitive model for *in vivo* evaluations. The experimental design was duly approved by the Committee for the Purpose of Control and Supervision of Experiments on Animals (CPCSEA) [Registration No. 379/01/ab/CPCSEA/02] of Dr. H. S. Gour Vishwavidyalaya, Sagar-470003 India. The Balb/c mice of uniform weight (20–25 g) were housed in ventilated plastic cages with access to water *ad libitum*. The mice were acclimatized at 25 ± 2 °C by maintaining the relative humidity (RH) 55–60% under natural light/dark condition prior to studies, avoiding any kind of stress on Balb/c mice.^{4,16,40–43}

2.13.2. Antitumor Targeting Efficacy Studies. The present antitumor targeting efficacy study was performed on tumor bearing Balb/c mice employing tumor growth inhibition study and Kaplan–Meier survival curve analysis. The tumor was developed on Balb/c mice using the well-known right flank method⁴ by injecting serum-free cultured MCF-7 cells in the

right hind leg of the mice. The development of tumor was regularly monitored by palpating the injected area with index finger and thumb. When the tumor grew to approximately 100 mm³ in size, mice were subjected to *in vivo* studies and Balb/c mice were accommodated in a pathogen-free laboratory environment.^{20,42,44} The sterilized free DOX, DOX/MWCNT, DOX/ox-MWCNT, DOX/PEG-MWCNT, DOX/FA-PEG-MWCNT, and DOX/ES-PEG-MWCNT formulations (equivalent dose = 5.0 mg/kg body weight) were intravenously administered into the mice through the tail vein route. The size of the tumor was measured using an electronic digital Vernier caliper and calculated using the formula = 1/2 × length × width². The median survival time was also recorded, and the study was terminated 45 days post treatment.

2.13.3. Pharmacokinetic and Biodistribution Studies after Intravenous Administration. The pharmacokinetic and biodistribution studies were performed on Balb/c mice after intravenous administration of the free DOX and DOX loaded MWCNT formulations (DOX/MWCNTs, DOX/ox-MWCNTs, DOX/ES-PEG-MWCNTs, DOX/FA-PEG-MWCNTs) at equivalent dose 5.0 mg/kg body weight dose. The blood was collected in to the Hi-Anticlot blood collecting vials (HiMedia, Mumbai, India) through retro-orbital plexus of the animal's eyes under mild anesthetic condition at the different time points. The collected blood was centrifuged after addition of 100 µL of trichloroacetic acid (TCA) in methanol (10% w/v) to separate RBCs. Supernatant was collected, vortexed, and ultracentrifuged (Z36HK, HERMLE LaborTechnik GmbH, Germany), and drug concentration was determined using the high performance liquid chromatography (HPLC) method. The pharmacokinetic parameters such as peak plasma concentration (C_{max}), the area under the curve (AUC_{0-t}), area under the first moment curve (AUMC), mean residence time (MRT), half-life ($t_{1/2}$), and half value duration (HVD) were also calculated.^{4,16,18,45}

The *in vivo* biodistribution study was also performed on tumor bearing Balb/c mice after administration of the same sterilized formulations. At 1, 6, 12, and 24 h time points mice were carefully sacrificed by the decapitation method. The different organs were separated out, washed with Ringer's solution for removal of any adhered debris, dried with tissue paper, weighed, and stored frozen until used. Weighed tissues samples were immediately homogenized (York Scientific Instrument, New Delhi, India), vortexed, and ultracentrifuged at 3000 rpm for 15 min (Z36HK, HERMLE LaborTechnik GmbH, Germany). The obtained clear supernatant was collected in HPLC vials and loaded onto the HPLC system to determine the concentration of DOX (Shimadzu, C18, Japan) using a mobile phase consisting of buffer pH 4.0/ acetonitrile/methanol (60:24:16; v/v/v) with 1.2 mL/min flow rate at 102/101 bar.^{41,46-49}

2.14. Statistical Analysis. The obtained data from the studies were presented as mean ± standard deviation ($n = 3$), and statistical analysis was performed using GraphPad InStat software (Version 6.00, Graph Pad Software, San Diego, California, USA) by one-way analysis of variance (ANOVA) followed by Tukey–Kramer multiple comparisons test. The comparison of the Kaplan–Meier survival analysis curve was performed using the Log-rank (Mantel–Cox) test (conservative). The pharmacokinetic data analysis of the plasma concentration time profile was conducted using the Kinetica 5.0 software (Thermo Scientific, USA), followed by non-compartmental analysis. A probability $p \leq 0.05$ was considered

significant while $p \leq 0.001$ was considered as extremely significant.

3. RESULTS AND DISCUSSION

The surface engineered smart, multifunctional carbon nanotubes appear to be useful in cancer chemotherapy as drug delivery systems, owing to their unique physicochemical properties and being continually explored in controlled and targeted drug delivery. As-synthesized pristine MWCNTs were procured and purified using different purification approaches rendering them suitable for further studies. The presence of impurities in pristine CNTs restricts their clinical application; thus emerges functionalization that renders them more biocompatible, safe, and effective for drug delivery. Functionalization is a well-known approach for surface alteration of CNTs. The f-MWCNTs used in the present investigation were prepared after proper functionalization and conjugation of targeting moieties, devoid of fluorescent dye, for cellular trafficking because doxorubicin has red-autofluorescence.

The FTIR spectrum of procured unmodified (pristine) MWCNTs depicts absorption peaks at 1626 and 2400.24 cm⁻¹. The characteristic peak at 1626 cm⁻¹ suggests the presence of carbon residue on the CNT surface, while a clear single characteristic peak at 2400.24 cm⁻¹ is ascribed to the stretching of the carbon nanotube backbone. The oxidized MWCNTs shows characteristic peaks approximately at 1637.4 and 3425.6 cm⁻¹ attributable to asymmetrical stretching of C=O stretching vibration mode and O–H stretching vibration, respectively.⁴

The FTIR spectrum of the FA-PEG-MWCNTs showed characteristic peaks at 1025.0, 3438.6, 2920.0, 1650.0, 1435.2, and 1320.5 cm⁻¹. The peaks at 1650.0 and 1435.2 cm⁻¹ of NH₂ stretching and O–H deformation of phenyl skeleton and a strong clear sharp characteristic peak observed at 1025.0 cm⁻¹ of C–O stretching of ether linkage suggest the attachment of FA-PEG to MWCNTs (Figure 1 A).

The estradiol conjugated with surface engineered MWCNTs shows the characteristic peaks in the range of 1500–1655 cm⁻¹ of –C=O anhydride and amide bonding of estradiol conjugated MWCNTs. A strong and sharp characteristic peak

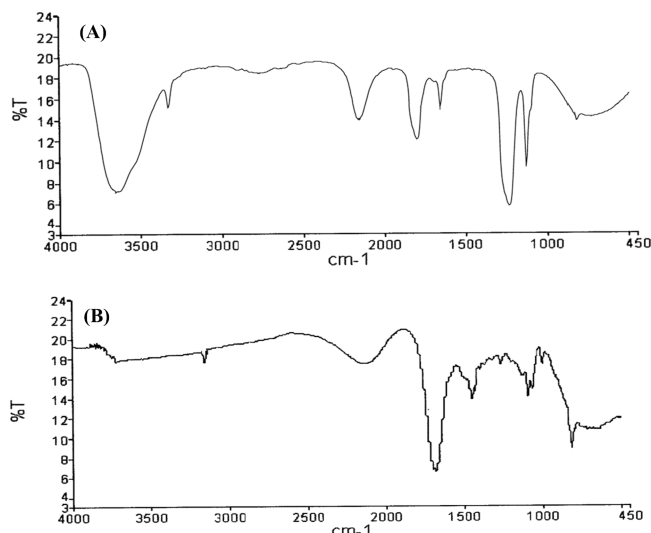
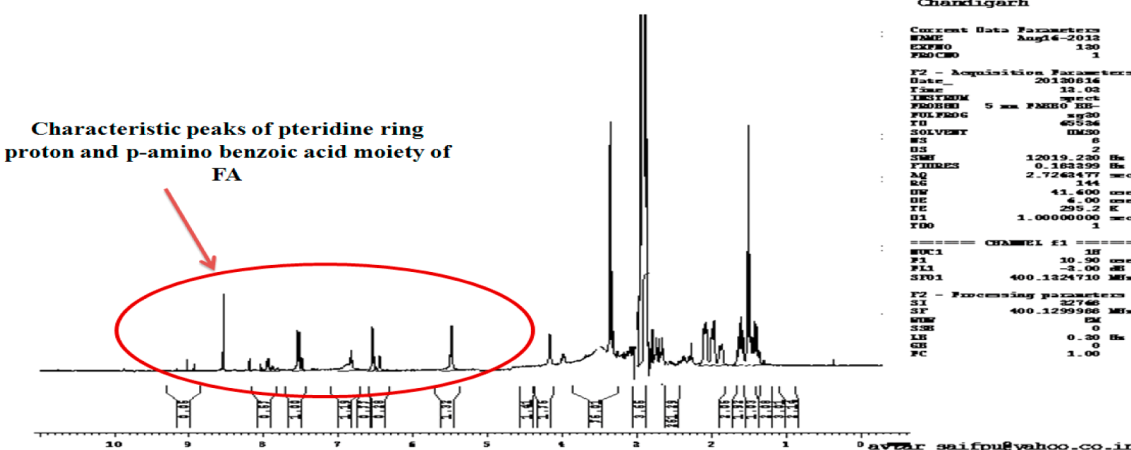


Figure 1. FTIR spectra of (A) FA-PEG-MWCNTs and (B) ES-PEG-MWCNTs.

(A) FA-PEG-MWCNTs



(B) ES-PEG-MWCNTs

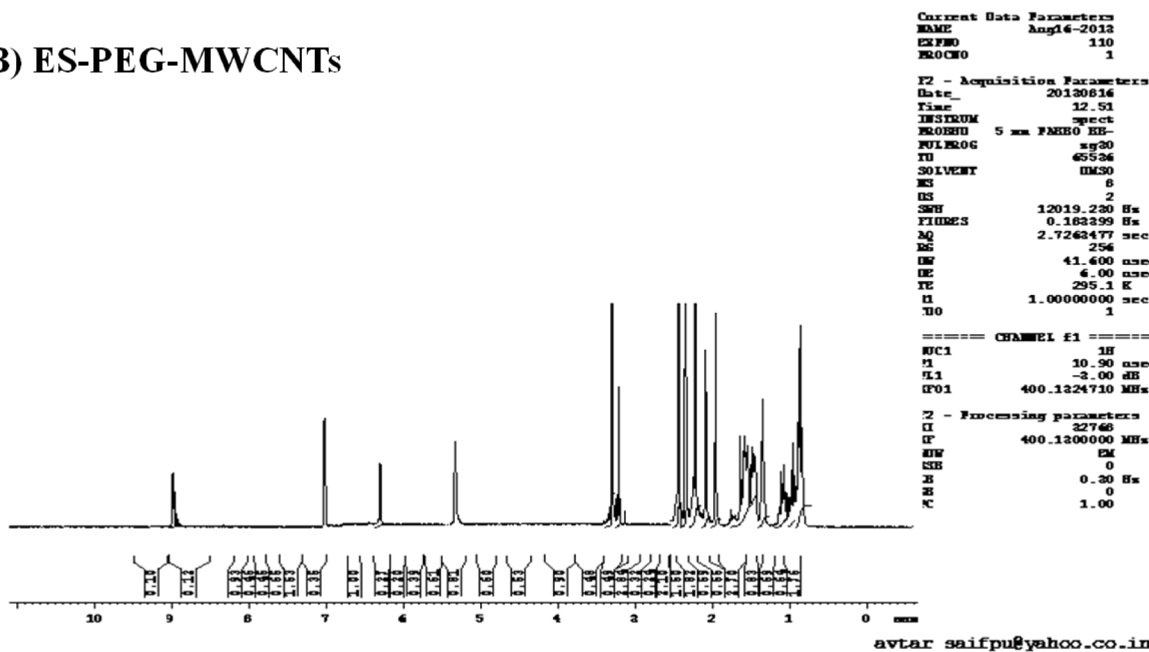


Figure 2. NMR spectra of (A) FA-PEG-MWCNTs and (B) ES-PEG-MWCNTs.

was found at 1020.04 cm^{-1} of C–O stretch of ether linkage due to the presence of polyether backbone of PEG. The characteristic peak at 1650.94 cm^{-1} of C–O stretching of amide bond formation clearly indicates confirmation of conjugation of estrone to MWCNTs (Figure 1 B).

The ¹H NMR spectra of the FA-PEG-MWCNTs and ES-PEG-MWCNTs are shown in Figures 2A and 2B. The characteristic signal of the pteridine ring proton and aromatic protons of the *p*-aminobenzoic acid (PABA) of FA was clearly present in the case of FA-PEG-MWCNTs (Figure 2 A). Similarly, ES-PEG-MWCNTs represent the protons characteristic of the phenyl ring of the steroid moiety showing chemical shifts as presented in the NMR spectrum (Figure 2 B).

Raman spectroscopy used for further characterization of the developed MWCNT conjugates provides information on hybridization state and defect site chemistry. It also gives information on changes in electronic structure upon anchoring of different chemical functional moieties. The MWCNTs show

the disorder related to D mode (approximately at $1330\text{--}1360\text{ cm}^{-1}$) and high-energy mode known as tangential G mode (approximately at $1500\text{--}1600\text{ cm}^{-1}$).⁴

Raman spectra of *ox*-MWCNTs, FA-PEG-MWCNTs, and ES-PEG-MWCNTs are shown in Figures 3A, 3B, and 3C. The Raman spectrum of *ox*-MWCNTs shows the Raman shifts at 1584.73 and 1352.0 cm^{-1} , which correspond to the G band (graphite-like mode) and D band (disorder-induced band), respectively (Figure 3 A). The Raman spectrum of the FA-PEG-MWCNTs shows the G band around 1565 cm^{-1} and D band around 1310 cm^{-1} (Figure 3 B). The Raman spectrum of the ES-PEG-MWCNTs shows the G band around 1580 cm^{-1} and D band around 1320 cm^{-1} (Figure 3 C). The shifting of G and D band intensity toward higher intensity in the case of FA-PEG-MWCNTs and ES-PEG-MWCNTs is mainly due to increase in the extent of conjugation of FA/ES-PEG- with functionalized MWCNTs, which would increase the single bond characteristics in the functionalized systems.

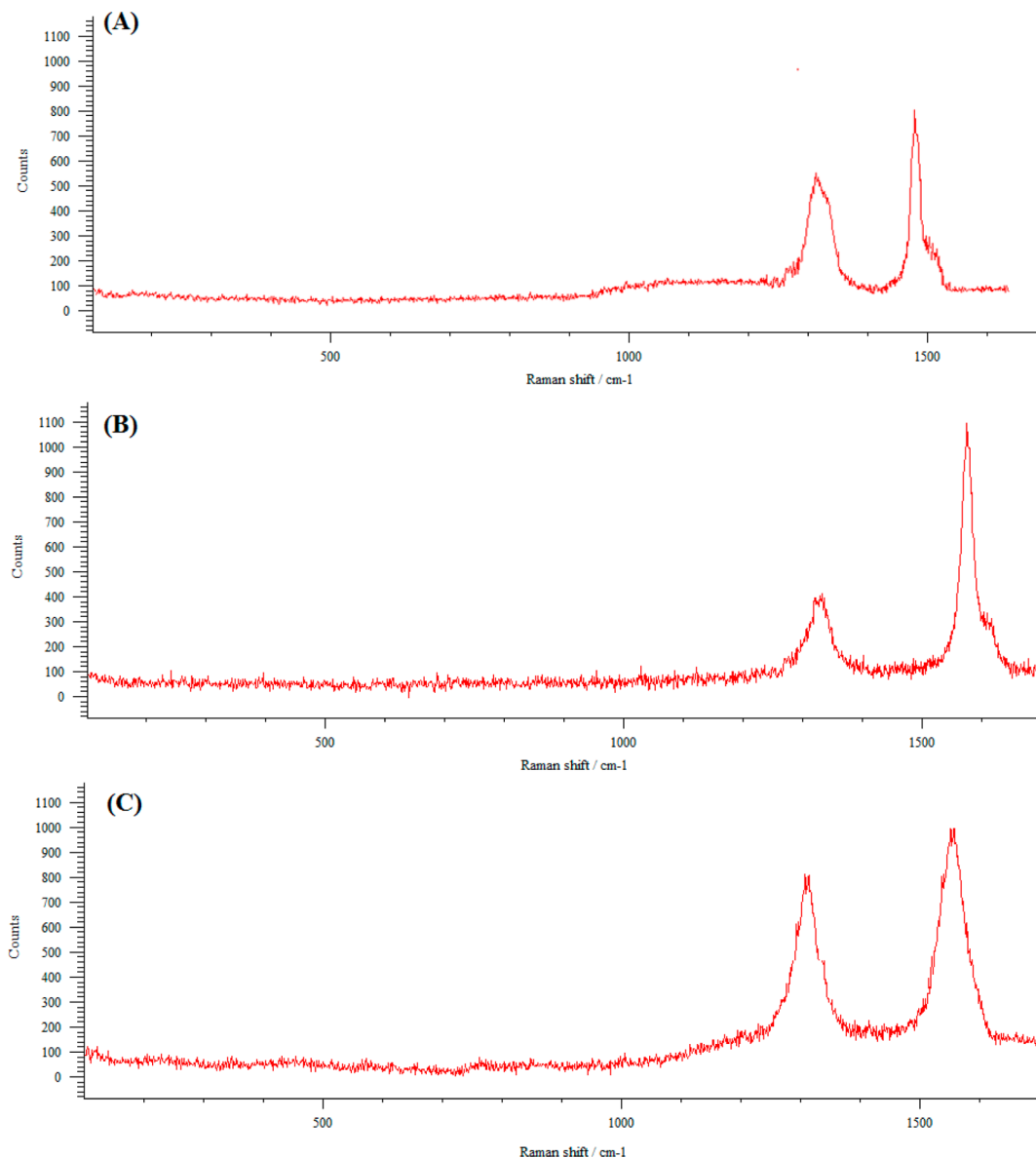


Figure 3. Raman spectra of (A) *ox*-MWCNTs, (B) ES-PEG-MWCNTs, and (C) FA-PEG-MWCNTs.

The transmission electron microscopy (TEM) clearly revealed that the developed formulations were in nanometric size range, even after conjugation.

The particle size and polydispersity index (PI) of the DOX/MWCNTs, DOX/*ox*-MWCNTs, DOX/FA-PEG-MWCNTs, and DOX/ES-PEG-MWCNTs were found to be 350.02 ± 5.24 , 230.12 ± 6.56 , 242.28 ± 5.85 , and 240.26 ± 4.50 and 0.22 ± 0.012 , 0.32 ± 0.023 , 0.55 ± 0.024 , and 0.85 ± 0.034 , respectively. The loading efficiency of DOX/MWCNTs, DOX/*ox*-MWCNTs, DOX/FA-PEG-MWCNTs, and DOX/ES-PEG-MWCNTs was calculated to be 92.50 ± 2.62 , 93.25 ± 3.52 , 96.50 ± 2.52 , and 96.80 ± 3.44 , respectively, and determined by absorption peak at 480.2 nm. A significant improvement in the loading efficiency was observed in the case of ligand conjugated MWCNTs through various interaction mechanisms (such as $\pi-\pi$ stacking, hydrogen bonding, and hydrophobic interactions) owing to the aromatic structure of the doxorubicin. Also large π -conjugated structures of the nanotubes can form $\pi-\pi$ stacking interaction with the quinine part of the DOX. One more possible reason is that cationically

charged DOX molecule could easily be adsorbed at lower potential of ES-/FA-PEG-MWCNTs than pristine and *ox*-MWCNTs via electrostatic interaction as well as $\pi-\pi$ stacking interaction that plays an important role with respect to DOX loading.^{2,4,15} Huang et al. reported approximately 91% of DOX loading efficiency in surface engineered SWCNTs.¹⁵ Similarly, the high surface area and conjugation chemistry of MWCNTs have been suggested to provide strong $\pi-\pi$ stacking interaction between CNTs and drug moieties.²⁵ According to Niu et al. DOX tends to strongly interact with side-walls of SWCNTs through $\pi-\pi$ stacking and hydrophobic interactions owing to their aromatic nature.¹⁰

The DOX released from known amounts of DOX/FA-PEG-MWCNTs, DOX/ES-PEG-MWCNTs, DOX/PEG-MWCNTs, DOX/*ox*-MWCNTs, and DOX/MWCNTs was determined separately in PBS (pH 7.4) and sodium acetate buffer solution (pH 5.3) up to 200 h. The obtained release pattern exhibited a nonlinear profile characterized by relatively faster initial release followed by sustained and slower release at later periods in both DOX/FA-PEG-MWCNT and DOX/ES-PEG-MWCNT for-

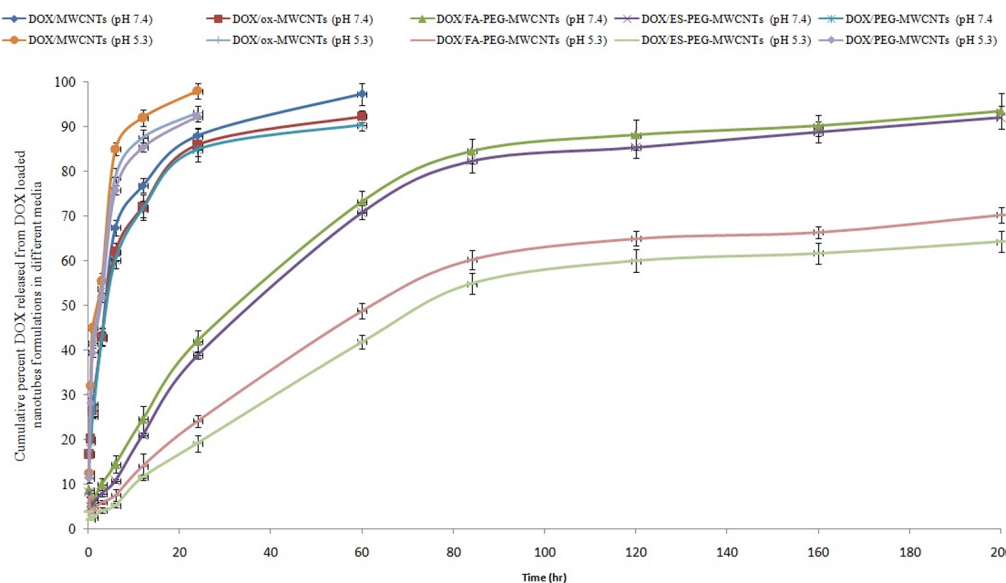


Figure 4. *In vitro* cumulative release behavior of DOX from developed carbon nanotube formulations at different pH conditions. Values represented as mean \pm SD ($n = 3$).

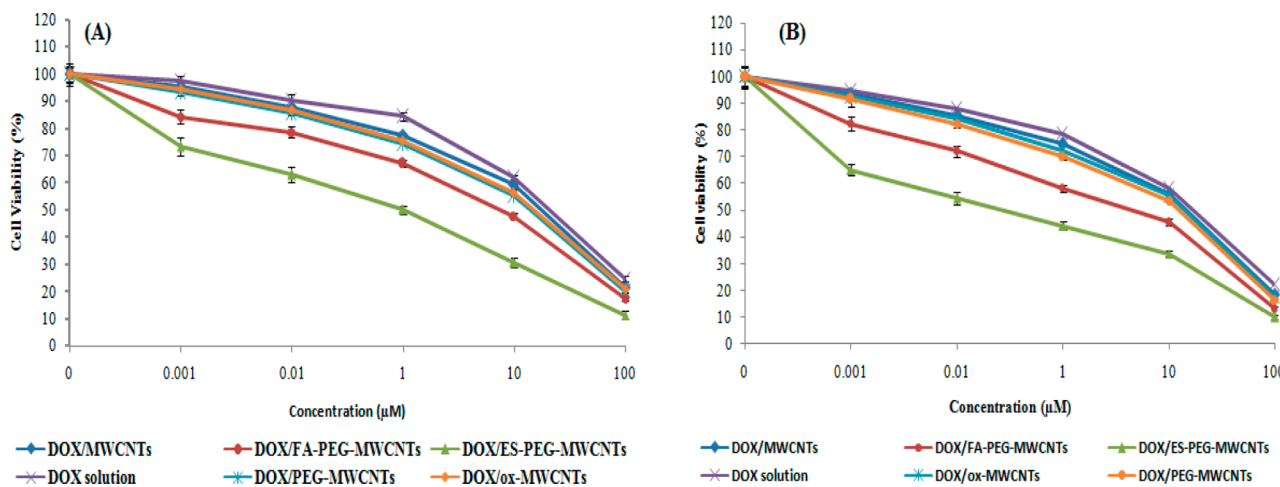


Figure 5. Percent cell viability of MCF-7 cells after treatment with free DOX, DOX/MWCNTs, DOX/ox-MWCNTs, DOX/PEG-MWCNTs, DOX/FA-PEG-MWCNTs, and DOX/ES-PEG-MWCNTs at (A) 24 and (B) 48 h ($n = 3$).

mulations (Figure 4). Moreover DOX/ox-MWCNTs and DOX/MWCNTs show faster release of DOX in both media. The release of DOX from the MWCNT formulation mainly depends on the solubility and pH of the media as well as the interaction and cleavage of bonding; an appreciable DOX release could be observed in an acidic pH solution, suggesting pH-dependent release. It is clearly observed that pH-dependent DOX release is beneficial in targeted drug delivery to cancerous cells. However, the DOX molecules stacked on the surface engineered MWCNT formulations are very stable in a neutral solution (pH 7.4) at 37 °C. This pH-triggered DOX release may be caused by a larger degree of protonation of the carboxyl ($-\text{COOH}$) and amino ($-\text{NH}_2$) groups on DOX at lower pH, which weakens the interaction between DOX and MWCNTs. At low pH, the hydrophilicity of DOX increases due to the protonation of the NH_2 groups native to its structure. The increased hydrophilicity aids in overcoming the interaction ($\pi-\pi$) among the DOX and the f-MWCNTs while facilitating its detachment from the nanotubes.^{4,14,15,51} Thus, the order of

release from MWCNT formulations at all pH ranges is as follows:



(Sustained Release)

Faster Release)

Zhang and co-workers reported pH-triggered drug release response from the modified nanotubes under normal physiological conditions and release at reduced pH, typical of microenvironments of intracellular lysosomes or endosomes and cancerous tissue.¹⁴ Our *in vitro* release data of DOX are in line with the previous reports.^{4,13–15,28}

The MTT assay was performed to determine the cancer targeting propensity of the DOX loaded nanotube formulations at 0.001, 0.01, 1, 10, and 100 μM concentration for 24 and 48 h treatment. The higher anticancer activity was achieved with targeting ligand anchored MWCNTs most probably due to the interaction of activated overexpressed estrone and folate receptors on the cell surface hence higher targeting ligand–receptor interaction affinity leading to apoptosis by intercalating DOX (anthracycline antibiotic) with DNA (Figure 5).

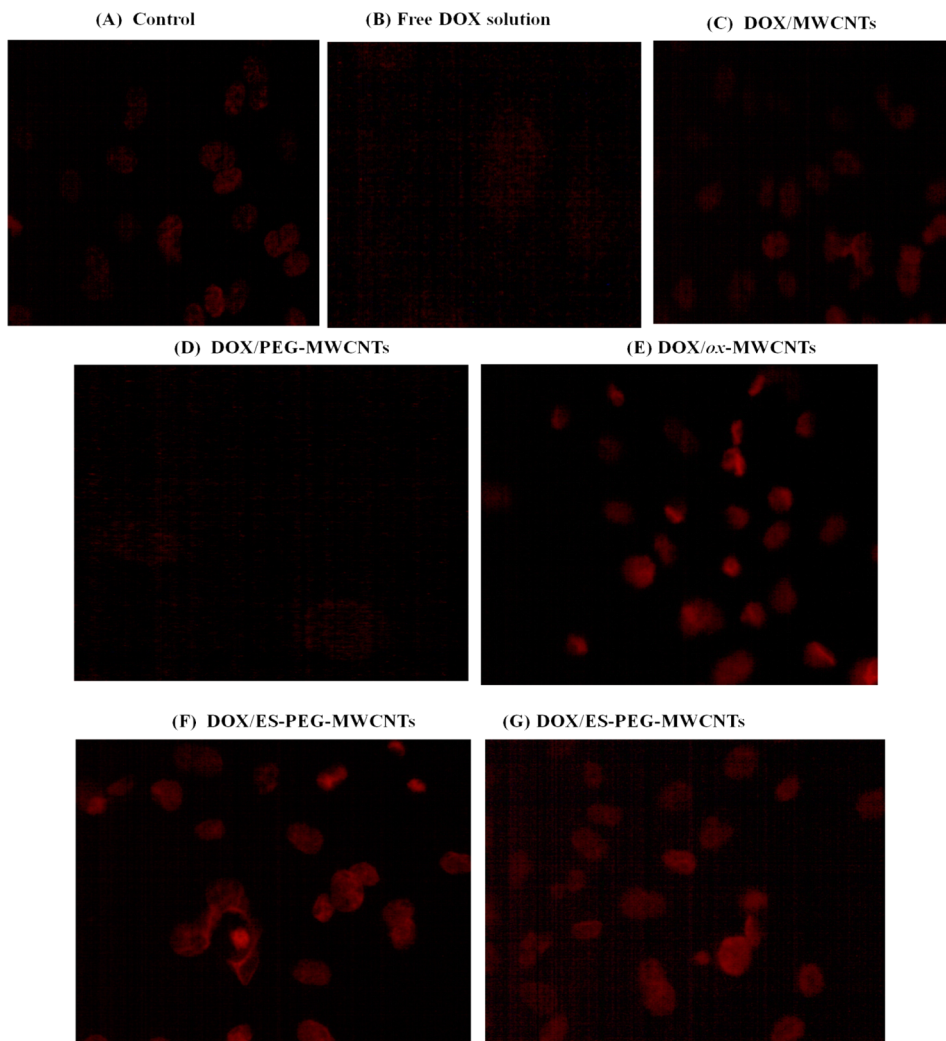


Figure 6. Fluorescent images of breast cancer MCF-7 cells of (A) control and after treatment with (B) free DOX, (C) DOX/MWCNTs, (D)DOX/PEG-MWCNTs, (E) DOX/ox-MWCNTs, (F) DOX/FA-PEG-MWCNTs, and (G) DOX/ES-PEG-MWCNTs (20 μ M concentration).

However, the nontargeted (DOX/MWCNTs and DOX/ox-MWCNTs) and PEGylated MWCNTs (DOX/PEG-MWCNTs) showed lesser cytotoxicity owing to low internalization in cancerous cells. The obtained results of cytotoxicity (MTT) assay are in good agreement with the previous published reports.^{14,27,33}

Flow cytometric analysis was used to determine the cellular uptake of the DOX loaded MWCNT formulations by MCF-7 cells. The cellular uptake efficiency was performed on MCF-7 cells after 3 h treatment with the different MWCNT formulations (free DOX, DOX/MWCNTs, DOX/ox-MWCNTs, DOX/PEG-MWCNTs, DOX/FA-PEG-MWCNTs, and DOX/ES-PEG-MWCNTs) and is shown in Figures 6 and 7. The fluorescence intensity of DOX/ES-PEG-MWCNTs, DOX/FA-PEG-MWCNTs, DOX/PEG-MWCNTs, DOX/ox-MWCNTs, DOX/MWCNTs, and free DOX was found to be 78.65, 78.12, 66.22, 62.46, 60.25, and 58.15%, respectively. The higher red fluorescence intensity was achieved in the case of targeting ligand-anchored MWCNT formulations compared to other formulations and control group. It is well reported that the DOX has red-autofluorescence intensity. In line with the cytotoxicity assay, cell uptake study also showed higher cellular uptake of the targeting ligand anchored nanotube formulations possibly due to the targeting ligand–receptor interactions

following receptor-mediated endocytosis and tiny nanoneedle specific mechanism and higher drug release. In spite of the high chemotherapeutic efficacy of DOX, clinical use is restricted due to its dose-limiting cardiotoxicity and renal and hepatic toxicity.

The overall high cellular uptake efficiency was ranked in the following order: DOX/ES-PEG-MWCNTs > DOX/FA-PEG-MWCNTs > DOX/PEG-MWCNTs > DOX/ox-MWCNTs > DOX/MWCNTs > free DOX > control.

The DNA cell cycle distribution study was performed to investigate the phases in which the developed nanotube formulations arrest the cancerous cells. The cell cycle analysis could be recognized by the four distinct phases in a proliferating cell population: G1, S, G2, and M phase.⁵⁰ The DOX/ES-PEG-MWCNTs showed 78.64%, 13.52%, and 11.22% cell arrest in G1, G2, and S phase, respectively. However, DOX/FA-PEG-MWCNTs showed 76.97%, 12.17%, and 10.86% cell arrest in G1, G2, and S phase, respectively. Thus, we conclude that the doxorubicin loaded MWCNT formulations were more efficient at attacking and killing the cancerous cells in the G1 phase, i.e., DNA synthesis by accumulation into nucleus. As it is well reported that the doxorubicin interacts with DNA by intercalation, thus the functions of DNA are affected and it is believed that the

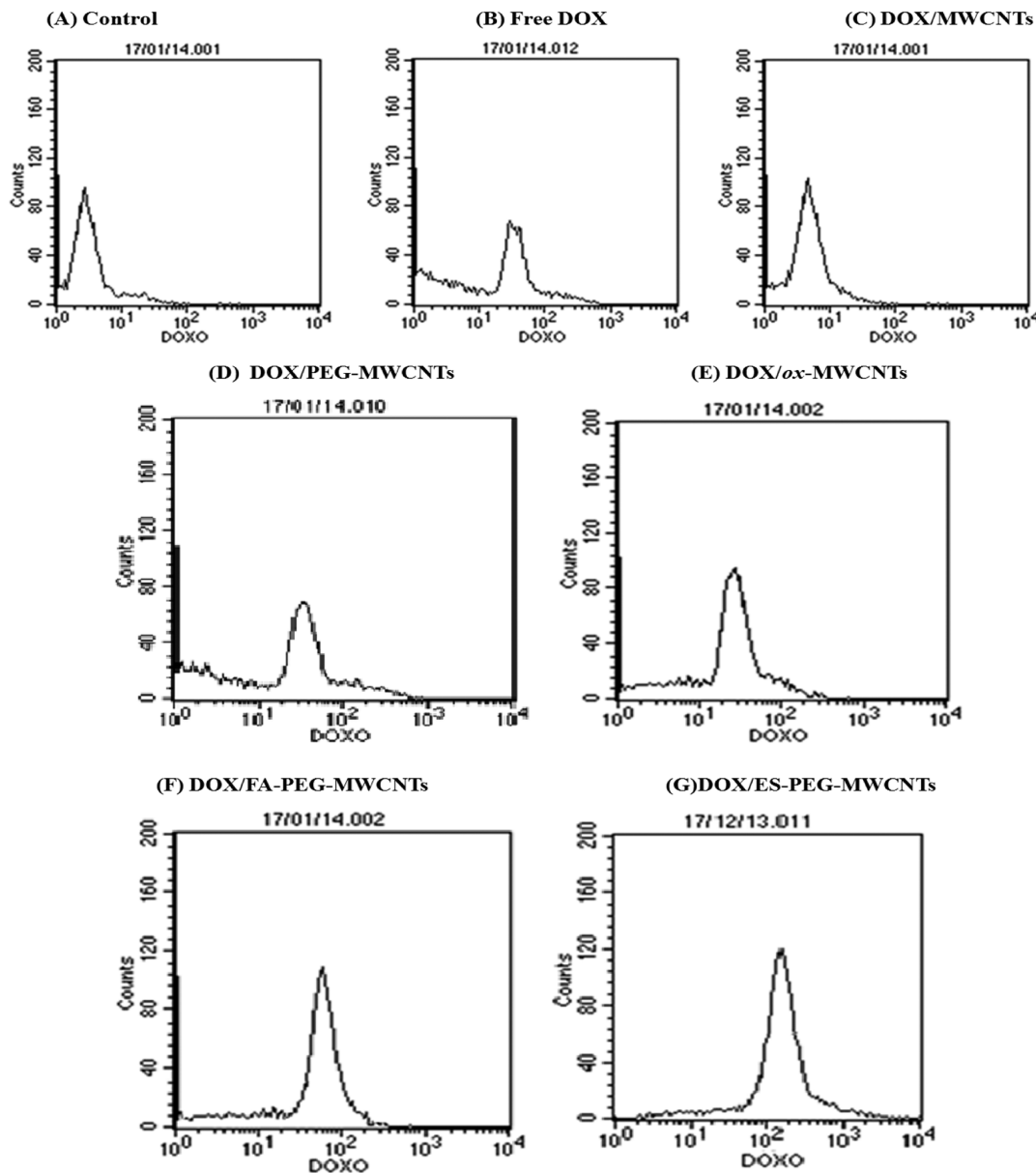


Figure 7. Quantitative cell uptake in breast cancer MCF-7 cells of (A) control and after treatment with (B) free DOX, (C) DOX/MWCNTs, (D) DOX/PEG-MWCNTs, (E) DOX/ox-MWCNTs, (F) DOX/FA-PEG-MWCNTs, and (G) DOX/ES-PEG-MWCNTs ($20 \mu\text{M}$ concentration).

Table 1. Pharmacokinetic Parameters of Free DOX, DOX/MWCNT, DOX/ox-MWCNT, DOX/PEG-MWCNT, DOX/FA-PEG-MWCNT, and DOX/ES-PEG-MWCNT Formulations^a

pharmacokinetic parameters	HVD (h)	$\text{AUC}_{0-t} (\mu\text{g}/\text{mL}\cdot\text{h})$	$\text{AUC}_{0-\infty} (\mu\text{g}/\text{mL}\cdot\text{h})$	$\text{AUMC}_{0-t} (\mu\text{g}/\text{mL}\cdot\text{h}^2)$	$\text{AUMC}_{0-\infty} (\mu\text{g}/\text{mL}\cdot\text{h}^2)$	$t_{1/2} (\text{h})$	MRT (h)
free DOX	0.3564 ± 0.04	9.3066 ± 0.08	9.3292 ± 0.22	21.6860 ± 0.26	22.0079 ± 0.22	1.5648 ± 0.01	2.3590 ± 0.01
DOX/MWCNTs	0.8329 ± 0.03	22.3127 ± 1.20	22.9233 ± 0.42	131.0810 ± 4.66	149.8770 ± 3.86	4.7022 ± 0.02	6.5381 ± 0.02
DOX/ox-MWCNTs	1.5208 ± 0.02	26.2936 ± 1.60	26.4129 ± 0.62	182.6100 ± 3.65	189.7500 ± 5.40	8.2596 ± 0.20	7.18397 ± 0.04
DOX/PEG-MWCNTs	0.9319 ± 0.02	27.3680 ± 6.68	28.5475 ± 7.88	265.1670 ± 8.26	295.996 ± 6.64	8.5706 ± 0.24	10.3685 ± 0.02
DOX/FA-PEG-MWCNTs	0.9318 ± 0.01	28.3430 ± 0.98	30.4799 ± 1.36	305.4730 ± 4.82	446.0940 ± 6.50	12.3431 ± 0.12	14.6357 ± 0.12
DOX/ES-PEG-MWCNTs	1.05418 ± 0.03	38.6518 ± 0.68	42.2180 ± 2.02	453.7930 ± 5.65	704.4600 ± 5.24	15.4495 ± 0.34	16.6863 ± 0.11

^aValues represented as mean \pm SD ($n = 3$). Abbreviations: C_{\max} = peak plasma concentration; T_{\max} = time taken to reach C_{\max} ; $t_{1/2}$ = elimination half-life; MRT = mean residence time; $\text{AUC}_{0-\infty}$ = area under plasma drug concentration over time curve; HVD = half value duration.

scission of DNA is mediated by binding of DOX to DNA and topoisomerase II enzyme.⁴

The pharmacokinetic parameters of DOX, DOX/ox-MWCNTs, DOX/MWCNTs, DOX/PEG-MWCNTs, DOX/

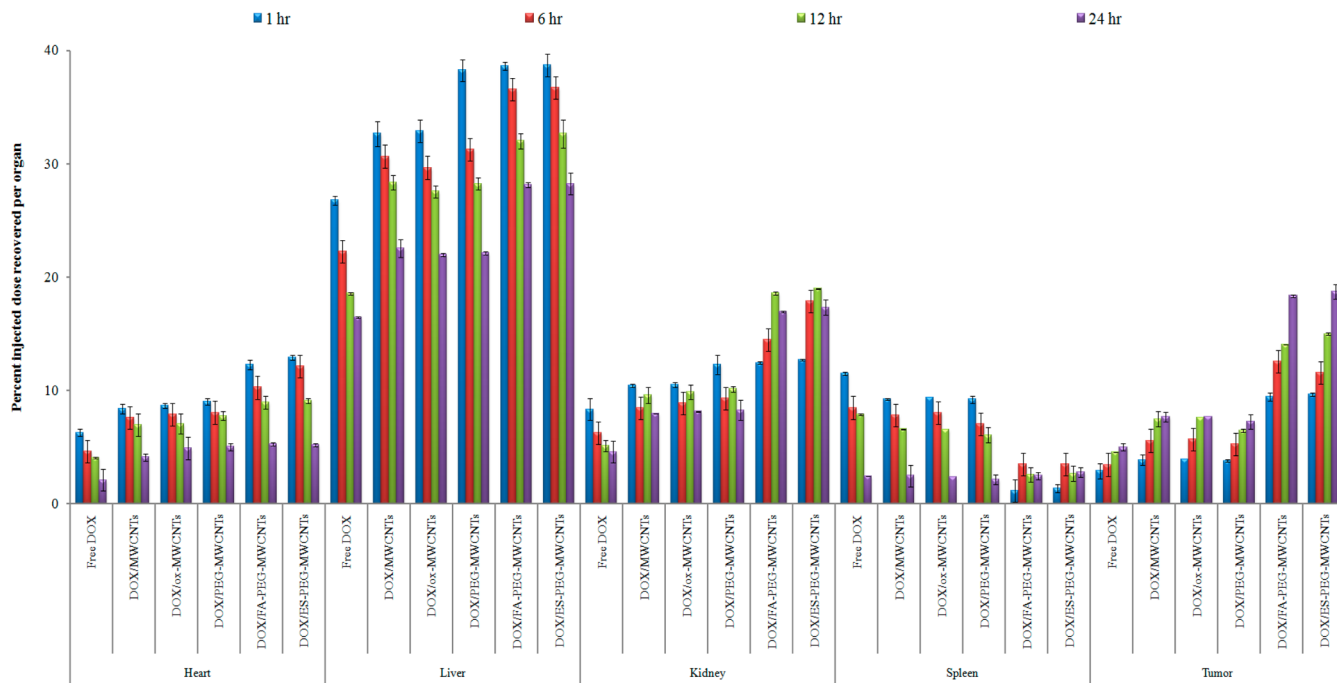


Figure 8. Biodistribution patterns of free DOX, DOX/MWCNT, DOX/ox-MWCNT, DOX/PEG-MWCNT, DOX/ES-MWCNT, and DOX/FA-PEG-MWCNT formulations in different tissues. Values represented as mean \pm SD ($n = 3$).

FA-PEG-MWCNTs, and DOX/ES-PEG-MWCNTs were investigated in the blood samples using the HPLC technique (Shimadzu, C18, Japan) after single iv administration in Balb/c mice (Table 1). The $AUC_{0-\infty}$ of DOX/ES-PEG-MWCNTs and DOX/FA-PEG-MWCNTs was 4.5-, 3.0-, and 1.8-, 1.2-fold higher compared to free DOX and DOX/MWCNTs, respectively. The $AUMC_{0-\infty}$ of DOX/ES-PEG-MWCNTs was 32-fold while MRT was found to be 7.07-fold higher compared to free DOX.

The average half-life ($t_{1/2}$) of DOX/ES-PEG-MWCNTs (15.4495 h) was 1.25, 1.80, 1.87, 3.28, and 9.87 times compared to DOX/FA-PEG-MWCNTs, DOX/PEG-MWCNTs, DOX/ox-MWCNTs, DOX/MWCNTs, and free DOX, respectively. However, MRT values of DOX/ES-PEG-MWCNTs were 1.14, 1.60, 2.32, 2.55, and 7.07 times compared to DOX/FA-PEG-MWCNTs, DOX/PEG-MWCNTs, DOX/ox-MWCNTs, DOX/MWCNTs, and free DOX, respectively (Table 1). The pharmacokinetic analysis results ascribed to the improved biocompatibility and increased pharmacokinetic of highly functionalized MWCNTs allow longer residence time inside the animal body and impart the stealth characteristic.

Liu et al. reported long-term fate of PEG functionalized SWCNTs after intravenous administration in animals and found longest blood circulation up to 1 day and nearly complete clearance of SWCNTs from the main organs approximately in 2 months. The intrinsic stability and structural flexibility of surface engineered CNTs may enhance the circulation time as well as the bioavailability of drug molecules.^{13,16}

In vivo biodistribution studies were performed on tumor bearing Balb/c mice after iv administration of the developed nanotube formulations, and highest DOX level was found in tumor, liver, and kidney in 24 h in the case of DOX/ES-PEG-MWCNTs. Both DOX/FA-PEG-MWCNT and DOX/ES-PEG-MWCNT formulations showed prolonged systemic circulation in blood after single iv administration, and level of

DOX recovered per organ is shown in Figure 8. The amount of DOX contents was found to be higher and accumulated significantly more in tumor tissue for ES-PEG and FA-PEG-MWCNTs compared to that of free DOX at all time points owing to the presence of targeting ligand and PEGylation. The acute cardiotoxicity is the main hurdle associated with doxorubicin chemotherapy. Thus, the concentration of DOX of the ligand anchored MWCNTs in the heart tissue was significantly lower than other nanotube formulations and efficiently delivered DOX at the target site through receptor-mediated endocytosis or tiny nanoneedle mechanisms. Higher amount of drug was delivered and accumulated at target sites by developed DOX/ES-PEG-MWCNTs formulations enhancing the therapeutic index with minimal toxicity to healthy/normal tissues like heart.

Antitumor activity of the different MWCNT formulations was evaluated in tumor bearing Balb/c model after single iv administration (5 mg/kg body weight). The DOX/ES-PEG-MWCNT, DOX/FA-PEG-MWCNT, DOX/PEG-MWCNT, DOX/ox-MWCNT, and free DOX formulations significantly suppressed tumor growth compared to control group. However, DOX/ES-PEG-MWCNT and DOX/FA-PEG-MWCNT formulations showed higher tumor growth suppression than other formulations and free drug solution (Figure 9 A). The high antitumor activity of the FA- and ES-PEG-conjugated MWCNTs can be attributed to its higher accumulation in cancer cells through receptor-mediated uptake. These antitumor activity results indicated that the PEGylation of CNTs increases the overall tumor targeting efficiency of the drug loaded ligand anchored MWCNT formulations.

The Kaplan–Meier survival curve analysis was used to measure the fraction of the treated mice that survived over a period of time. It is the simplest way of computing the survival over time. The time starting from a defined point to the occurrence of a given event, for example death, is called survival

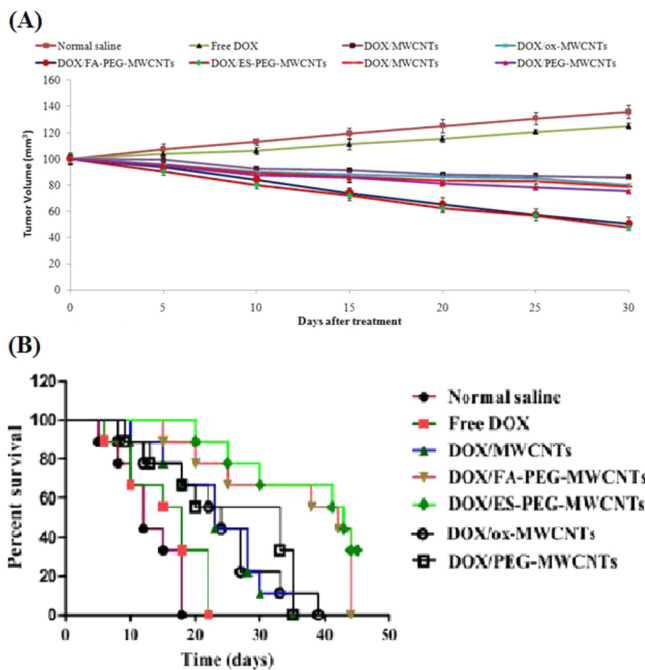


Figure 9. (A) Tumor regression analysis and (B) Kaplan–Meier survival curves of MCF-7 bearing Balb/c mice analyzed by Log-rank (Mantel–Cox) after intravenous administration of free DOX, DOX/MWCNT, DOX/PEG-MWCNT, DOX/ox-MWCNT, DOX/FA-PEG-MWCNT, and DOX/ES-PEG-MWCNT formulations at 5.0 mg/kg body weight dose, where **p* ≤ 0.05, ***p* ≤ 0.01, and ****p* ≤ 0.001.

time, and the analysis of group data is called survival analysis.^{2,4,42}

Survival periods were plotted between percent survival and days elapsed to assess the effectiveness of developed MWCNT formulations. Survival curves show, for each time plotted on the *x*-axis, the portion of all individuals surviving at that time and regularly monitored in the separate group up to 45 days. The Kaplan–Meier survival curves suggested that the median survival time for tumor bearing mice treated with DOX/ES-PEG-MWCNTs (43 days) was extended compared to DOX/FA-PEG-MWCNTs (42 days), DOX/PEG-MWCNTs (33 days), DOX/ox-MWCNTs (24 days), DOX/MWCNTs (23 days), free DOX (18 days), and control group (12 days). The DOX/ES-PEG-MWCNTs has also shown significantly longer survival span (43 days) than DOX/FA-PEG-MWCNTs (42 days), DOX/PEG-MWCNTs (33 days), free DOX (18 days), and control group (12 days) as shown in Figure 9B. Our antitumor targeting activity results are in good agreement with the previously published reports.^{2,4,42}

4. CONCLUSION

At present the functionalized MWCNTs are the most widely explored new generation targeted drug delivery system. The cancer targeting potential of the different targeting chemical moieties, i.e., estrone (ES) and folic acid (FA) anchored MWCNTs, has been validated in the present investigation. In this debut attempt, we have compared and explored the one-platform comparative studies utilizing two targeting ligand anchored surface engineered MWCNTs employing doxorubicin (anthracycline antibiotic; anticancer agent) on MCF-7 cells. The ligand anchored MWCNT formulations exhibit higher loading efficiency, anticancer activity, and improved biocompat-

ability profile along with increased pharmacokinetic parameters compared to free drug solution. From the findings we conclude that the overall pharmaceutical cancer targeting efficacy of MWCNTs formulations utilizing MCF-7 cells ranked in the following order: DOX/ES-PEG-MWCNTs > DOX/FA-PEG-MWCNTs > DOX/PEG-MWCNTs > DOX/ox-MWCNTs > DOX/MWCNTs > free DOX > control. Thus, estrone anchored MWCNTs show superior targetability compared to FA-anchored, oxidized (*ox*), plain MWCNTs, and free DOX solution. In the future we wish to explore the various other drug loaded targeting ligand anchored CNTs in the search of a safer and more effective nanomedicine.

■ AUTHOR INFORMATION

Corresponding Author

*Tel/fax: + 91-7582-265055. E-mail: jnarendr@yahoo.co.in.

Notes

The authors declare no competing financial interest.

■ ACKNOWLEDGMENTS

One of the authors (N.K.M.) is thankful to University Grants Commission (UGC), New Delhi, for providing the Senior Research Fellowship during the tenure of the studies. The authors also acknowledge Department of Physics, Dr. H. S. Gour University, Sagar, India, for Raman spectroscopy; All India Institute of Medicine and Sciences (AIIMS), New Delhi, India (TEM); Indian Institute of Technology (IIT), Indore (AFM), India; Central Instruments Facilities (CIF), National Institute of Pharmaceutical Education and Research (NIPER), Mohali, Chandigarh, India; Central Drug Research Institute (CDRI), Lucknow; Diya Laboratory, Mumbai, India. The authors are also thankful to National Centre for Cell Sciences (NCCS), Pune, India, for providing the MCF-7 cell lines.

■ REFERENCES

- (1) Mehra, N. K.; Jain, N. K. Functionalized Carbon Nanotubes and Their Drug Delivery Applications; Bhoop, B. S., Ed.; Studium Press, LLC: London, 2014; Vol. 4, pp 327–369.
- (2) Mehra, N. K.; Jain, N. K. Development, characterization and cancer targeting potential of surface engineered carbon nanotubes. *J. Drug Targeting* 2013, 21 (8), 745–758.
- (3) Iijima, S. Helical microtubules of graphitic carbon. *Nature* 1991, 354, 56–58.
- (4) Mehra, N. K.; Verma, A. K.; Mishra, P. R.; Jain, N. K. The cancer targeting potential of D- α -tocopheryl polyethylene glycol 1000 succinate tethered multi walled carbon nanotubes. *Biomaterials* 2014, 35, 4573–4588.
- (5) Jain, K.; Mehra, N. K.; Jain, N. K. Potential and emerging trends in nanopharmacology. *Curr. Opin. Pharmacol.* 2014, 15, 97–106.
- (6) Ali-Boucetta, H.; Kostarelos, K. Pharmacology of carbon nanotubes: Toxicokinetics, excretion and tissue accumulation. *Adv. Drug Delivery Rev.* 2013, 65, 2111–2119.
- (7) Fan, J.; Zeng, F.; Xu, J.; Wu, S. Targeted anti-cancer prodrug based on carbon nanotube with photodynamic therapeutic effect and pH-triggered drug release. *J. Nanopart. Res.* 2013, DOI: 10.1007/s11051-013-1911-z.
- (8) Jain, A. K.; Mehra, N. K.; Lodhi, N.; Dubey, V.; Mishra, D.; Jain, N. K. Carbohydrate-conjugated multiwalled carbon nanotubes: development and characterization. *Nanomedicine* 2009, 5 (4), 432–442.
- (9) Lacerda, L.; Russier, J.; Pastorini, G.; Herrero, M. A.; Venturelli, E.; Dumortier, H.; Al-Jamal, K. T.; Prato, M.; Kostarelos, K.; Bianco, A. Translocation mechanisms of chemically functionalized carbon nanotubes across plasma membranes. *Biomaterials* 2012, 33, 3334–3343.

- (10) Niu, L.; Meng, L.; Lu, Q. Folate-conjugated PEG on single-walled carbon nanotubes for targeting delivery of doxorubicin to cancer cells. *Macromol. Biosci.* **2013**, *13*, 735–744.
- (11) Fabbro, C.; Ali-Boucetta, H.; Ros, T. D.; Kostarelos, K.; Bianco, A.; Prato, M. Targeting carbon nanotubes against cancer. *Chem. Commun.* **2012**, *48*, 3911–3926.
- (12) Mehra, N. K.; Mishra, V.; Jain, N. K. A review of ligand tethered surface engineered carbon nanotubes. *Biomaterials* **2014**, *35* (4), 1267–1283.
- (13) Liu, Z.; Sun, X.; Nakayama-Ratchford, N.; Dai, H. Supramolecular chemistry on water soluble carbon nanotubes for drug loading and delivery. *ACS Nano* **2007**, *1* (1), 50–56.
- (14) Zhang, X.; Meng, L.; Lu, Q.; Fei, Z.; Dyson, P. J. Targeted delivery and controlled release of doxorubicin to cancer cells using modified single wall carbon nanotubes. *Biomaterials* **2009**, *30*, 6041–6047.
- (15) Huang, H.; Yuan, Q.; Shah, J. S.; Misra, R. D. K. A new family of folate-decorated and carbon nanotubes-mediated drug delivery system: synthesis and drug delivery response. *Adv. Drug Delivery Rev.* **2011**, *63*, 1332–1339.
- (16) Liu, Z.; Chen, K.; Davis, C.; Sherlock, S.; Cao, Q.; Chen, X.; Dai, H. Drug delivery with carbon nanotubes for in vivo cancer treatment. *Cancer Res.* **2008**, *68* (16), 6652–6660.
- (17) Mody, N.; Tekade, R. K.; Mehra, N. K.; Chopdey, P.; Jain, N. K. Dendrimer, liposomes, carbon nanotubes and PLGA nanoparticles: one platform assessment of drug delivery potential. *AAPS PharmSciTechnol* **2014**, *15* (2), 388–399.
- (18) Singh, R.; Mehra, N. K.; Jain, V.; Jain, N. K. Folic acid conjugated carbon nanotubes for gemcitabine HCL delivery. *J. Drug Targeting* **2013**, *21* (6), 581–592.
- (19) Wu, W.; Wieckowski, S.; Pastorin, G.; Benincasa, M.; Klumpp, C.; Briand, J. P. Targeted delivery of Amphotericin B to cells by using functionalized carbon nanotubes. *Angew. Chem., Int. Ed.* **2005**, *44*, 6358–6362.
- (20) Bhatnagar, I.; Venkatesan, J.; Kim, S.-K. Polymer functionalized single walled carbon nanotubes mediated drug delivery of Gliotoxin in cancer cells. *J. Biomed. Nanotechnol.* **2014**, *10* (1), 120–130.
- (21) Gupta, R.; Mehra, N. K.; Jain, N. K. Fucosylated multiwalled carbon nanotubes for Kupffer cells targeting for the treatment of cytokine-induced liver damage. *Pharm. Res.* **2013**, *31* (2), 322–334.
- (22) Wu, L.; Man, C.; Wang, H.; Lu, X.; Ma, Q.; Cai, Y.; Ma, W. PEGylated multi-walled carbon nanotubes for encapsulation and sustained release of oxaliplatin. *Pharm. Res.* **2013**, *30*, 412–423.
- (23) Paliwal, S. R.; Paliwal, R.; Pal, H. C.; Saxena, A. K.; Sharma, P. R.; Gupta, P. N.; Agrawal, G. P.; Vyas, S. P. Estrogen-anchored pH-sensitive liposomes as nanomodule designed for site-specific delivery of doxorubicin in breast cancer therapy. *Mol. Pharmaceutics* **2012**, *9* (1), 176–186.
- (24) Lodhi, N.; Mehra, N. K.; Jain, N. K. Development and characterization of dexamethasone mesylate anchored on multi walled carbon nanotubes. *J. Drug Targeting* **2013**, *21* (1), 67–76.
- (25) Lu, Y. J.; Wei, K. C.; Ma, C. C. M.; Yang, S. Y.; Chen, J. P. Dual targeted delivery of doxorubicin to cancer cells using folate-conjugated magnetic multi-walled carbon nanotubes. *Colloids Surf., B* **2012**, *89*, 1–9.
- (26) Mehra, N. K.; Mishra, V.; Jain, N. K. Receptor based therapeutic targeting. *Ther. Delivery* **2013**, *4* (3), 369–394.
- (27) Das, M.; Singh, R. P.; Datir, S. R.; Jain, S. Intracellular drug delivery and effective in vivo cancer therapy via estradiol-PEG-appended multi walled carbon nanotubes. *Mol. Pharmaceutics* **2013**, *10* (9), 3404–3416.
- (28) Das, M.; Singh, R. P.; Datir, S. R.; Jain, S. Surface chemistry dependent “switch” regulated the trafficking and therapeutic performance of drug-loaded carbon nanotubes. *Bioconjugate Chem.* **2013**, *24*, 626–639.
- (29) Zalipsky, S.; Gilon, C.; Zalkha, A. Attachment of drugs to polyethylene glycols. *Eur. Polym. J.* **1983**, *19*, 1177–1183.
- (30) Rai, S.; Paliwal, R.; Vyas, S. P. Targeted delivery of doxorubicin via estrone-appended liposomes. *J. Drug Targeting* **2008**, *16* (6), 455–463.
- (31) Lee, R. J.; Low, P. S. Folate-mediated tumor cell targeting of liposome entrapped doxorubicin in vitro. *Biochim. Biophys. Acta* **1995**, *1233*, 134–144.
- (32) Kesharwani, P.; Tekade, R. K.; Jain, N. K. Formulation development and in vitro–in vivo assessment of the fourth-generation PPI dendrimer as a cancer-targeting vector. *Nanomedicine* **2014**, *9* (15), 2291–2308 DOI: 10.2217/nmm.13.210.
- (33) Lee, P. C.; Chiou, Y. C.; Wong, J. M.; Peng, C. L.; Shieh, M. J. Targeting colorectal cancer cells with single-walled carbon nanotubes conjugated to anticancer agent SN-38 and EGFR antibody. *Biomaterials* **2013**, *34*, 8756–8765.
- (34) Nima, Z. A.; Mahmood, M. W.; Karmakar, A.; Mustafa, T.; Bourdo, S.; Xu, Y.; Biris, A. S. Single-walled carbon nanotubes as specific targeting and Raman spectroscopic agents for detection and discrimination of single human breast cancer cells. *J. Biomed. Opt.* **2013**, *18* (5), 55003.
- (35) Sacchetti, C.; Rapini, N.; Magrini, A.; Cirelli, E.; Bellucci, S.; Matteri, M.; Rosato, N.; Bottini, N.; Bottini, M. In vivo targeting of intracellular regulatory T cell using PEG-modified single-walled carbon nanotubes. *Bioconjugate Chem.* **2013**, *24*, 852–858.
- (36) Delogu, L. G.; Venturelli, E.; Manetti, R.; Pinna, G. A.; Carru, C.; Madeddu, R.; Murgia, L.; Sgarrella, F.; Dumortier, H.; Bianco, A. Ex vivo impact of functionalized carbon nanotubes on human immune cells. *Nanomedicine* **2012**, *7* (2), 231–243.
- (37) Chen, J.; Li, S.; Shen, Q. Folic acid and cell-penetrating peptide conjugated PLGA-PEG bifunctional nanoparticles for vincristine sulfate delivery. *Eur. J. Pharm. Sci.* **2012**, *47*, 430–443.
- (38) Han, Y.; Xu, J.; Li, Z.; Ren, G.; Yang, Z. In vitro toxicity of multi-walled carbon nanotubes in C6 rat glioma cells. *Neurotoxicology* **2012**, *33*, 1128–1134.
- (39) Kundu, P.; Mohanty, C.; Sahoo, S. K. Anti-glioma activity of curcumin-loaded lipid nanoparticles and its enhanced bioavailability in brain tissue for effective glioblastoma therapy. *Acta Biomater.* **2012**, *8*, 2670–2687.
- (40) Mulvey, J. J.; Villa, C. H.; MCDevitt, M. R.; Escoria, F. E.; Casey, E.; Scheinberg, D. A. Self-assembly of carbon nanotubes and antibodies on tumours for targeted amplified delivery. *Nat. Nanotechnol.* **2013**, *8*, 763–771.
- (41) Lin, Z.; Xi, Z.; Huang, J. Biodistribution of single-walled carbon nanotubes in rats. *Toxicol. Res.* **2014**, DOI: 10.1039/C3TX50059D.
- (42) Ren, J.; Shen, S.; Wang, D.; Xi, Z.; Guo, L.; Pang, Z.; Qian, Y.; Sun, X.; Jiang, X. The targeted delivery of anticancer drugs to brain glioma by PEGylated oxidized multi-walled carbon nanotubes modified with angiopoep-2. *Biomaterials* **2012**, *33*, 3324–3333.
- (43) Ji, Z.; Lin, G.; Lu, Q.; Meng, L.; Shen, X.; Dong, L.; Fu, C.; Zhang, X. Targeted therapy of SMMC-7721 liver cancer in vitro and in vivo with carbon nanotubes based drug delivery systems. *J. Colloid Interface Sci.* **2012**, *365*, 143–149.
- (44) Muscella, A.; Vertugno, C.; Migoni, D.; Biagioli, F.; Fanizzi, F. P.; Fornai, F.; De Pascali, S. A.; Marsigliante, S. Antitumor activity of [Pt (O,O'-acac) (γ -acac)] (DMS) in mouse xenograft model of breast cancer. *Cell Death Dis.* **2014**, *5*, e1014.
- (45) Cherukuri, P.; Gannon, C. J.; Leeuw, T. K.; Schmidt, H. K.; Smalley, R. E.; Curley, S. A.; Weisman, R. B. Mamalian pharmacokinetics of carbon nanotubes using intrinsic near-infrared fluorescence. *Proc. Natl. Acad. Sci. U.S.A.* **2006**, *103* (50), 18882–18886.
- (46) Al-Jamal, K. T.; Nunes, A.; Methven, L.; Ali-Boucetta, H.; Li, S.; Toma, F. M.; Herrero, M. A.; Al-Jamal, W. T.; Eikelder, H. M. M.; Foster, J.; Mather, S.; Prato, M.; Bianco, A.; Kostarelos, K. Degree of chemical functionalization of carbon nanotubes determines tissue distribution and excretion profile. *Angew. Chem., Int. Ed.* **2012**, *51*, 6389–6393.
- (47) Bhirde, A.; Patel, V.; Gavard, J.; Zhang, G.; Sousa, A. A.; Masedunskas, A.; Leapman, R. D.; Weigert, R.; Gutkind, J. S.; Rusling, J. F. Targeted killing of cancer cells in vivo and in vitro with EGF-

directed carbon nanotubes-based drug delivery. *ACS Nano* **2009**, *3* (2), 307–316.

(48) Campagnolo, L.; Massimiani, M.; Palmieri, G.; Bernardini, R.; Sacchetti, C.; Bergamaschi, A. Biodistribution and toxicity of pegylated single wall carbon nanotubes in pregnant mice. *Part. Fibre Toxicol.* **2013**, DOI: 10.1186/1743-8977-10-21.

(49) Jain, S.; Thakare, V. S.; Das, M.; Godugu, C.; Jain, A. K.; Mathur, R.; Chuttani, K.; Mishra, A. K. Toxicity of multi walled carbon nanotubes with end defects critically depends on their functionalization density. *Chem. Res. Toxicol.* **2011**, *24* (11), 2028–2040.

(50) Nunez, R. DNA measurement and cell cycle analysis by flow cytometry. *Curr. Issues Mol. Biol.* **2001**, *3* (3), 67–70.

(51) Dinan, N. M.; Atyabi, F.; Rouini, M. R.; Amini, M.; Golbchifar, A. K.; Dinarvand, R. Doxorubicin loaded folate-targeted carbon nanotubes: preparation, cellular internalization, in vitro cytotoxicity and disposition kinetic study in the isolated perfused rat liver. *Mater. Sci. Eng. C* **2014**, *39*, 47–55.